

ANNUAL REPORT
COMPREHENSIVE RESEARCH ON RICE
January 1, 2009– December 31, 2009

PROJECT TITLE:

Study of Rice for Improved Quality and Processing Efficiency

PROJECT LEADER:

Zhongli Pan
Department of Biological and Agricultural Engineering
University of California, Davis
One Shields Ave
Davis, CA 95616

Processed Food Research Unit
USDA ARS WRRC
800 Buchanan St.
Albany, CA 94710

PRINCIPAL INVESTIGATORS:

Zhongli Pan
Department of Biological and Agricultural Engineering
University of California, Davis
One Shields Ave
Davis, CA 95616

Processed Food Research Unit
USDA ARS WRRC
800 Buchanan St.
Albany, CA 94710

James F. Thompson
Department of Biological and Agricultural Engineering
University of California – Davis
One Shields Ave.
Davis, CA 95616

LEVEL OF 2009 FUNDING: \$29,900

OBJECTIVES AND EXPERIMENTS CONDUCTED, BY LOCATION, TO ACCOMPLISH OBJECTIVES:

Our previous research has demonstrated that rice could be dried at high temperatures with much reduced time and high milling quality when infrared radiation heating was used. At the same time, it is also evidenced that M206 is more fissure resistant than M202, which could be due to the differences in physical structures and chemical composition of rice kernels. A better understanding of the drying mechanism and the differences between varieties could help in developing new drying methods and breeding of new fissure resistant varieties. To achieve these goals, we have selected the following specific objectives:

1. Investigate the moisture distribution in rice kernels using magnetic resonance imaging.
2. Compare drying rates of rice varieties M202 and M206.
3. Compare sorption characteristics of rice components of M202 and M206 varieties.
4. Develop sorption isotherm model to predict equilibrium moisture content of rice varieties M202 and M206.
5. Investigate distribution of carbohydrates, lipids and proteins in rice kernels using scanning electron microscopy.
6. Investigate structure of rice kernel using X-Ray Imaging and scanning electron microscope.

SUMMARY OF 2009 RESEARCH (major accomplishments), BY OBJECTIVE:

Moisture distribution in rice kernels determined using magnetic resonance imaging (MRI)

Rice drying was normally studied in bulk quantities. Little emphasis was given to how moisture changes inside an individual kernel during this process. However, this information is necessary in determining moisture gradients developed within the kernel. These moisture gradients are believed to cause fissuring in rice and thus, lower rice quality.

Measuring moisture distribution inside a rice kernel experimentally has always been very difficult, mainly due to its small size. However, with recent advances in MRI technique, the moisture distribution inside the rice kernel can be observed with high resolution. We used a 9.4 Tesla instrument at NMR facility at UC Davis for this study. We were able to get a resolution of 0.1 – 0.5 mm in our images which means about 15 data points along the shortest axis of rice kernel. We scanned images of rice kernel at regular intervals during the drying process and the obtained image data were then analyzed using MATLAB™ (Mathworks Inc., Natick, MA). Drying experiments were conducted at 20, 25 and 43°C and Californian M206 rice variety was used.

Single rough rice kernel was placed in the MRI equipment for this experiment. A typical set of images, which were taken at the start of the drying experiment, is shown in Figure 1. It shows the signal intensity along the sixteen parallel slices taken in transverse plane of the kernel. Due to the sample holder a ring is seen in each figure. In this experiment, the space imaged was 8 mm long, 8 mm wide and 8 mm thick. Each pixel in the image represents a signal intensity corresponding

to volume of 0.125 mm by 0.125 mm in transverse plane and 0.5 mm in longitudinal axis direction. Red color denotes higher signal intensity whereas a blue color indicates smaller.

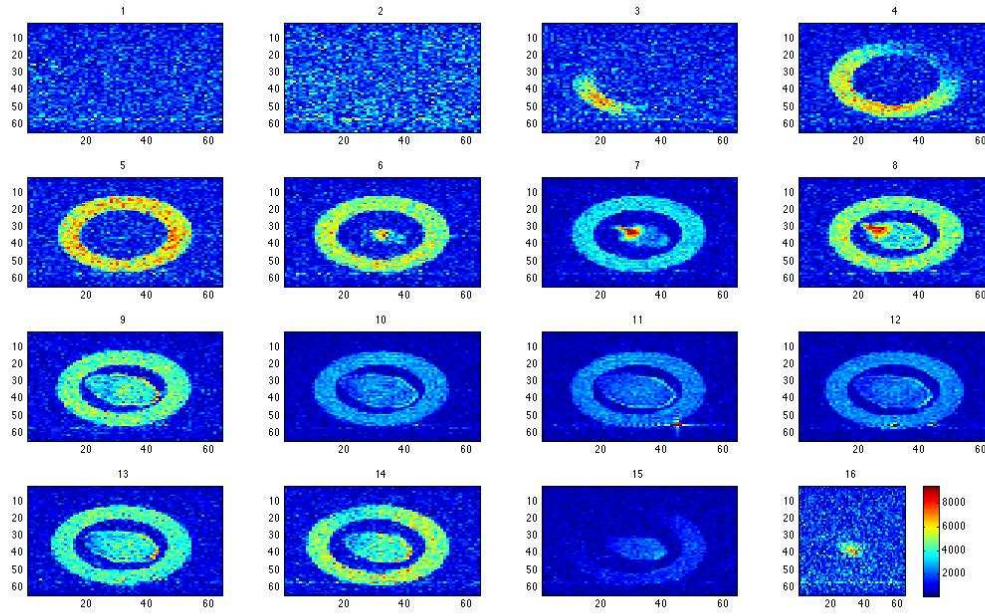


Figure 1. MRI Signal intensity of sixteen slices at start of drying

In first five images, only noise signal is visible as size of kernel was smaller than the space imaged by the instrument. Signal intensity is proportional to the moisture and the fat content. The high signal intensity (intense red region in slice 4, 5 and 6 in Figure 1) was due to high fat content in those regions. Since fat content does not change during the drying process, difference in signal intensity with time is an indicator of moisture loss. To achieve this, one image is subtracted from the other, pixel by pixel where each pixel has a numeric value that corresponds to a signal intensity (represented by colors in graphical drawings). Such plots are called subtraction plots. Figure 2 shows such plot, where each row of images represents all sixteen slices at given time subtracted from corresponding slice of the initial image when drying has just begun. This figure indicates the moisture differences between original rice and dried rice (at specific locations) at drying time of 9, 32, 60, 85 and 111 minutes with 43 °C and 0.40 m³/h air flow rate over the single kernel.

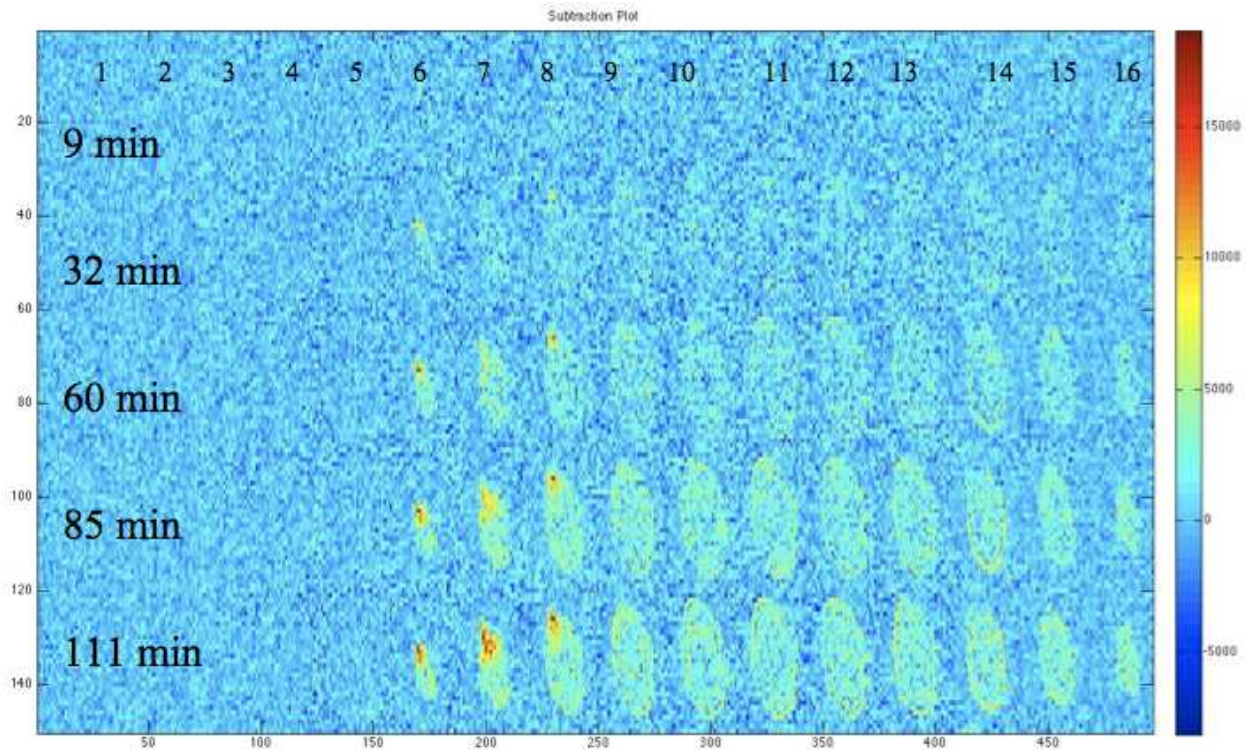


Figure 2. Subtraction plots of all sixteen slices for 9, 32, 60, 85 and 111 minutes of drying

Moisture loss in the sixth, seventh and eighth slices, in each row was higher than the rest of the slices. In reality, this corresponds to the region of rice that contains the embryo. The red regions visible in these slices show that moisture removal rate is higher at this location compared to other regions. Similar trends were observed during drying at 20 °C and 25 °C temperatures. This is the first time that different regions inside the kernel have been observed to dry at different rates. These findings need to be further confirmed by bulk drying methods.

Drying rates of Rice varieties M202 and M206

Higher drying rates i.e. faster moisture removal from kernels may cause larger moisture gradients and hence, can cause rice to fissure. To identify the differences in drying rates of varieties M202 and M206, both were dried at 25 °C and 45 °C by convective air drying methods. Drying curves are shown in **Figure 3** and **Figure 4**, respectively. Rice samples for these experiments were grown in identical field conditions. Harvest moisture content of M206 was 18.2 % and of M202 was 22.4 % on wet basis (or 22.2 % and 28.9% on dry basis). It is known that drying rate depends upon initial moisture content, therefore, prior to main drying experiments, M202 variety, having higher initial moisture content, was slowly dried by ambient air drying method until both M202 and M206 had roughly equal moisture contents. After this slow drying, in order to have uniform moisture distribution within the kernels, samples were allowed to equilibrate in plastic ziplock bags at ambient temperature of 25 °C.

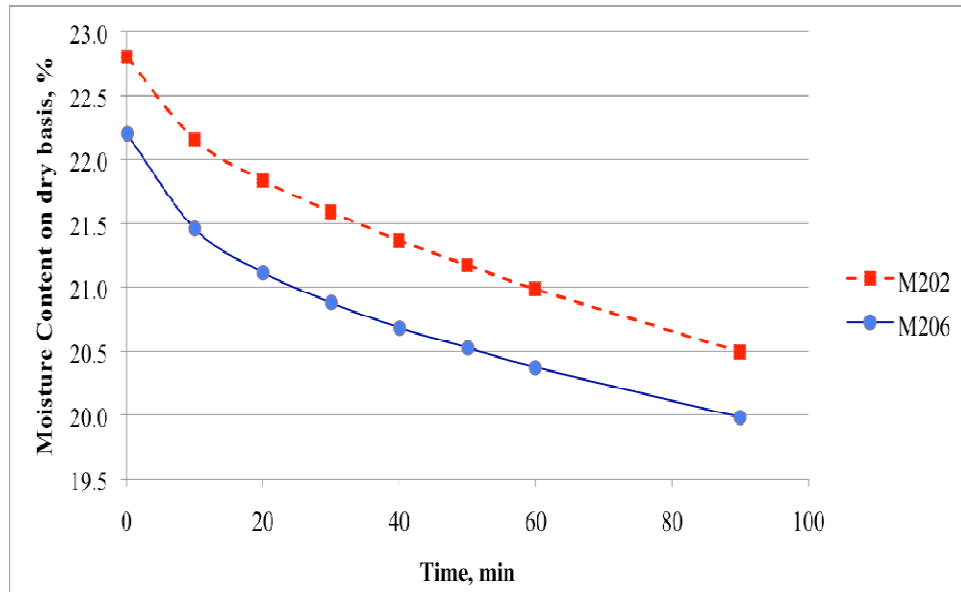


Figure 3. Drying curve of rice varieties M202 and M206 during air drying at 25 °C

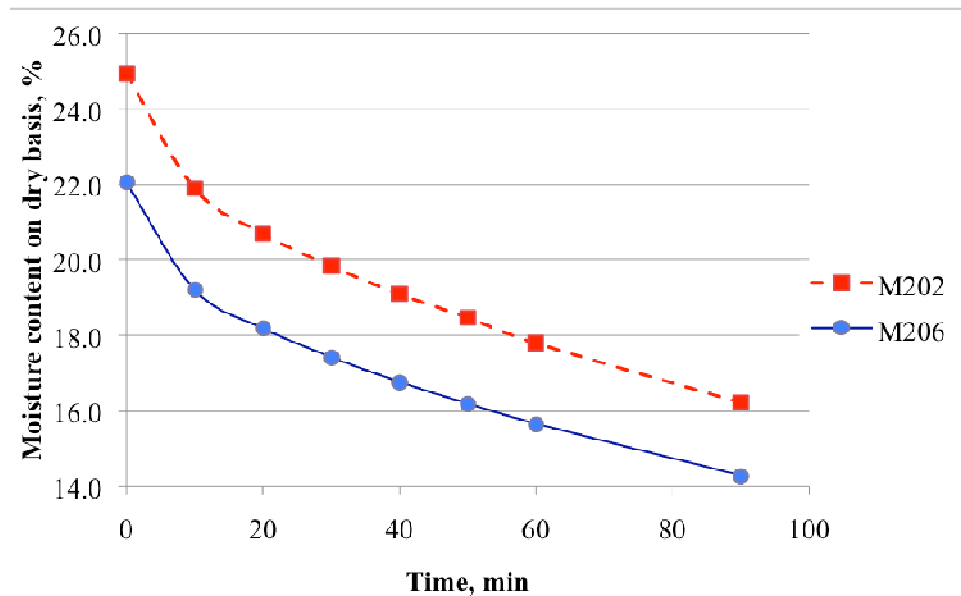


Figure 4. Drying curve of rice varieties M202 and M206 during air drying at 45 °C

Figure 3 and

Figure 4 show that drying curves of both varieties are almost parallel, meaning that their drying rates are similar. Moisture removal in same drying time differed by less than 10%. This means moisture gradients developed during these drying conditions are alike. Apart from drying, the moisture gradients can also develop in field and during handling and storage, when exposed to humid or dry conditions. To understand the differences in moisture absorption and desorption during these conditions, sorption experiments were conducted. Results of these experiments are presented in the next section.

Sorption characteristics of rice components

The sorption isotherm characteristics of M202 and M206 have been determined experimentally and have been further characterized according to the Brunauer *et al.* (1940) classification, who classified the adsorption isotherms into five general types. For interpretation purposes, sorption isotherm for a typical food system might be divided into three main regions as shown in Figure 5.

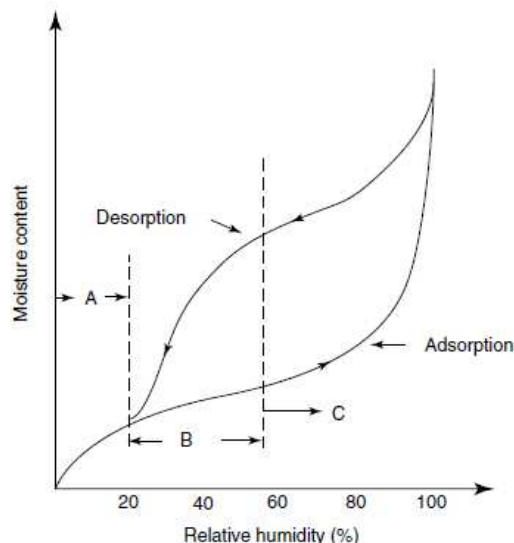


Figure 5. Sorption isotherm for a typical food product.

In Figure 5, region A represents strongly bound water with an enthalpy of vaporization considerably higher than that of pure water. Usually water molecules in this region are unfreezable and are not available for chemical reactions or as plasticizers. Region B, represents water molecules which are less firmly bound and available as a solvent for low molecular weight solutes and for some biochemical reactions. In region C or above, excess water is present in macro-capillaries and exhibits nearly all the properties of bulk water. The water is capable of acting as a solvent and microbial growth becomes a major deteriorative reaction in this region.

A Dynamic Vapor Sorption (DVS Advantage-1, Surface Measurement Systems, PA, USA) was used to obtain sorption isotherm characteristics of rough, brown and white rice and the husk. DVS equipment uses compressed nitrogen as the carrier gas and works in the temperature range of 5 to 60°C with 0.1°C sensitivity and in the relative humidity range of 0-98% with 1% sensitivity. The rice kernels were stored at 4°C prior to experiments. The rice kernels that fall into a certain weight range were used for experiments, which are given in

Table 1. For each experiment, three rice kernels of M202 or M206 or parts of rice husk from at least three different rice grains were placed into the pan of the equipment. The relative humidity was changed from 0 to 97.9 to 0% at 20% R.H. steps and the temperature was kept constant at 25°C which is in line with the conditions selected with different authors (Roman-Gutierrez et al., 2002; Arlabosse et al. 2003).

Table 1. Weight (mg) of the selected rice kernels for DVS experiments (The data is reported as mean \pm SD)

	M202	M206
<i>Rough rice</i>	30.06 \pm 0.80	31.14 \pm 0.50
<i>Brown Rice</i>	24.57 \pm 0.71	25.02 \pm 0.72
<i>White Rice</i>	20.97 \pm 0.47	22.30 \pm 0.57

The sorption isotherms for rough, brown and white rice and husk for M202 and M206 varieties are presented in Figs. 6, 8 - 10. For each type of rice and variety, hysteresis was observed. Hysteresis is generally observed in most hygroscopic products. A product is called hygroscopic if it is able to bind water when the vapor pressure is lowered. The degree of hysteresis was more significant for rough and brown rice, than white rice and husk. It was also observed that, absorption isotherms exhibited lower moisture content than the desorption isotherms at a given relative humidity, possibly due to the hygroscopic nature of rice kernels.

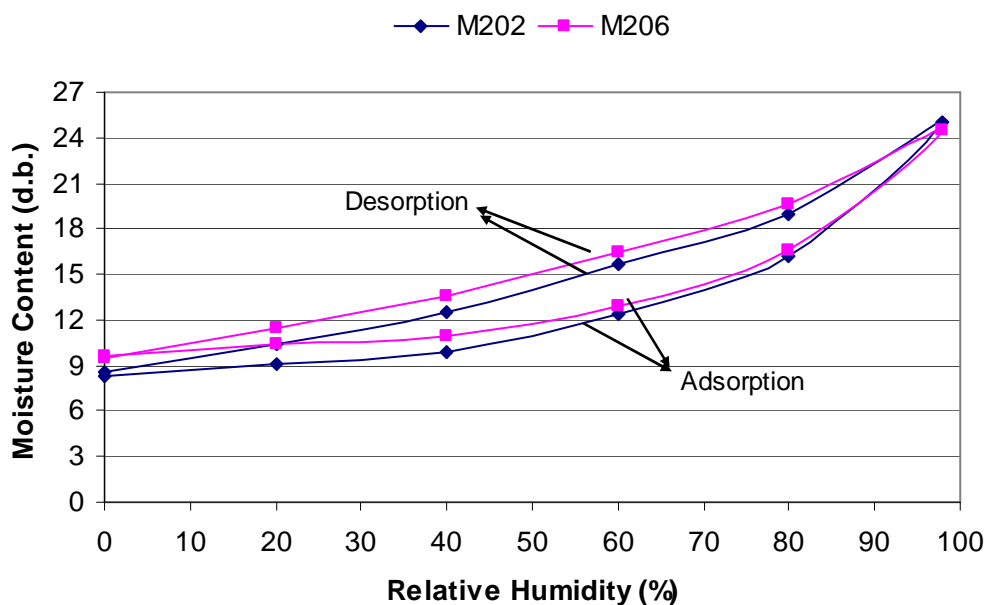


Figure 6. Sorption isotherm of rough rice for M202 and M206

It is seen in Figure 6 that the isotherms for M202 and M206 are similar in nature where both varieties show type 3 isotherm characteristics according to the Brunauer *et al.* (1940) classification. It is also observed that at 0% RH, M202 can be dried to lower moisture contents than do M206. Although both isotherms are similar in nature, it is worth to look at absorption characteristics of both varieties at 97.9 % RH, which is shown in Figure 7.

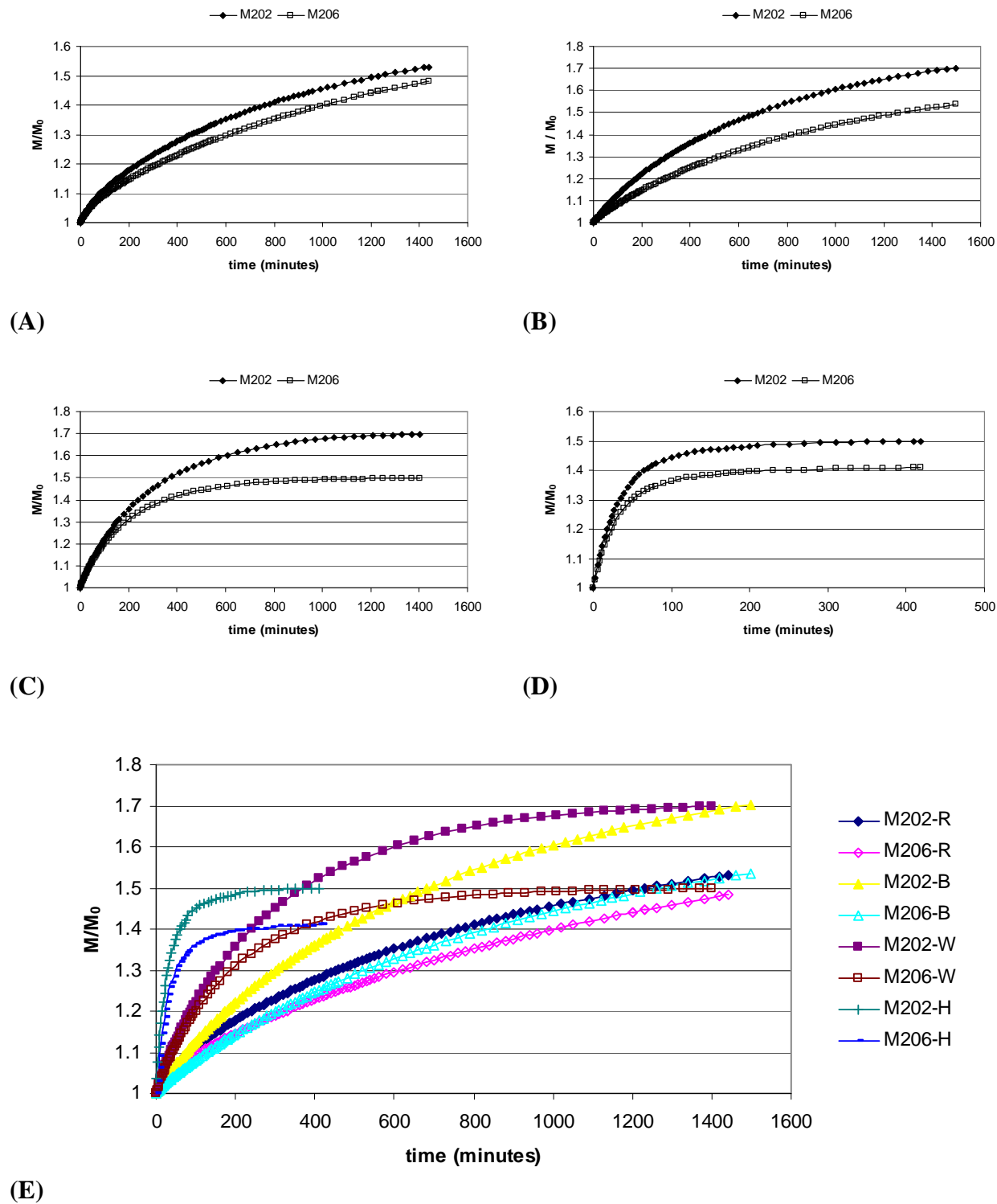


Figure 7. Absorption characteristic of (A) rough rice, (B) brown rice, (C) white rice, (D) husk and (E) all components, of M202 and M206 at 97.9% relative humidity

It is clearly seen from Figure 7 that for all rice fractions, M202 absorbs moisture faster than M206, which might make it more susceptible to fissuring at moisture adsorbing environments such as combine hopper, field cart, transport truck or holding bin. Among the different components, order of absorption rate is husk > white rice > brown rice > rough rice.

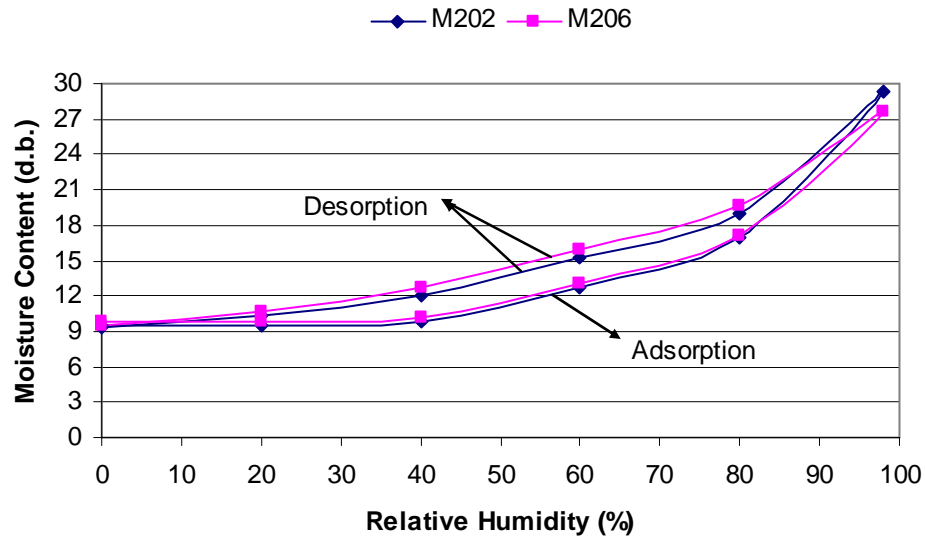


Figure 8. Sorption isotherms of brown rice for M202 and M206

It is seen from Figure 6 and Figure 8 that below 10% moisture content (d.b.), the water in rice represents strongly bound water with an enthalpy of vaporization considerably higher than pure water. This is more profound in brown rice than rough rice where the husk of the rough rice might be playing a role in changing the sorption characteristics.

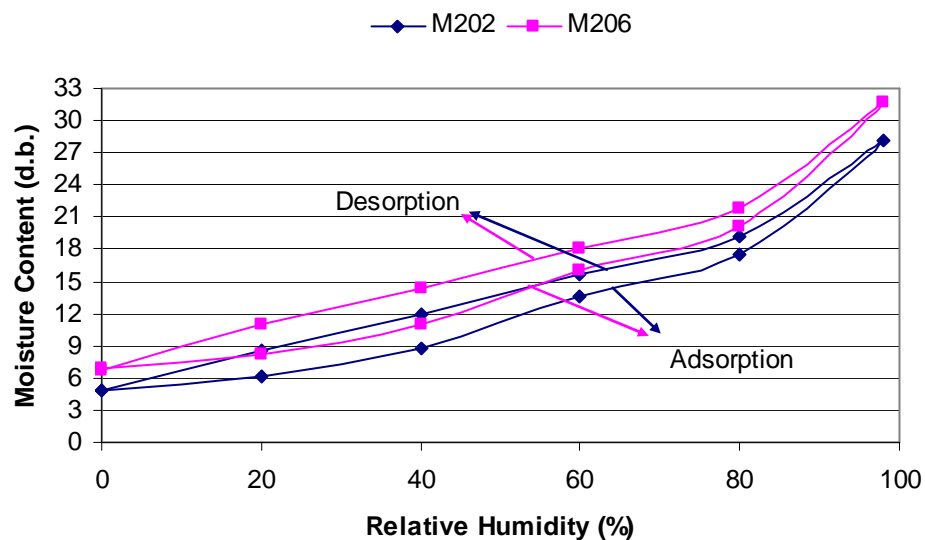


Figure 9. Sorption isotherms of white rice for M202 and M206

It is seen in Figure 9 that both varieties show type 2 isotherms according to the Brunauer *et al.* (1940) classification. It was observed that above 80% relative humidity there was significant increase in moisture absorption and desorption characteristics of both varieties.

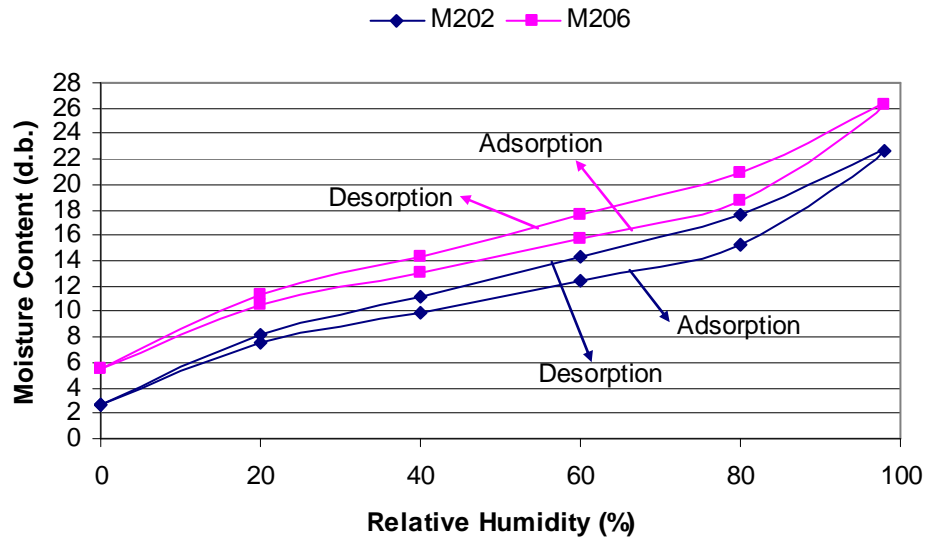


Figure 10. Sorption isotherms of husk of M202 and M206

It is seen from Figure 10 that the shape of the isotherm is close to type 5 isotherms. This is especially observed when the solid is porous thus having an internal surface, so that the thickness of the adsorbed layer on the walls of the pores is necessarily limited by the size of the pores. This is confirmed by SEM image of M206 husk that is shown in Figure 11, where the porous structure of husk is clearly visible.

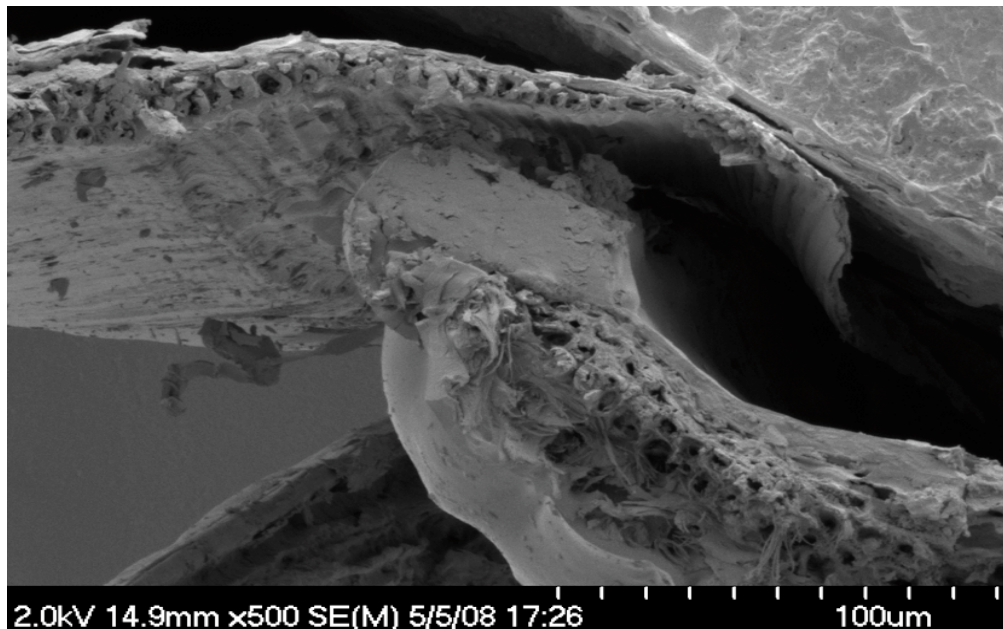


Figure 11. Porous structure of rice husk

The moisture content (d.b.) values of different rice types for M202 and M206 variety, presented in Figs. 6, 8-10 is tabulated in Table 2. The moisture content values other than the presented values in Table 2, can be found using the mathematical model described in the following section.

Table 2: Equilibrium moisture content of different rice components at selected relative humidities (a – absorption, d – desorption; R- rough rice, B- brown rice, W- white rice, H-husk)

	Relative Humidity (%)										
	0a	20a	40a	60a	80a	97.9a	80d	60d	40d	20d	0d
M202-R	8.35	9.15	9.82	12.36	16.21	24.99	19.02	15.73	12.53	10.39	8.57
M206-R	9.64	10.38	10.99	12.96	16.60	24.46	19.65	16.44	13.53	11.46	9.50
M202-B	9.45	9.43	9.78	12.68	16.88	29.36	18.99	15.32	12.04	10.26	9.33
M206-B	9.85	9.83	10.12	13.01	17.10	27.59	19.58	15.94	12.66	10.72	9.46
M202-W	4.91	6.11	8.76	13.57	17.48	28.10	19.28	15.69	11.99	8.65	4.76
M206-W	6.82	8.22	10.91	15.98	20.20	31.76	21.84	18.13	14.32	10.95	6.67
M202-H	2.72	7.48	9.91	12.50	15.31	22.64	17.57	14.32	11.16	8.24	2.72
M206-H	5.49	10.51	13.02	15.76	18.64	26.26	20.95	17.62	14.33	11.31	5.54

Prediction of equilibrium moisture content by sorption isotherm models

The data obtained corresponding to water activity, a_w , and moisture content (d.b.), m , at the studied temperature were fitted to GAB (Guggenheim, Anderson, de Boer) model. QtiPlot software, which uses Scaled Levenberg-Marquardt algorithm and which is distributed under GNU General Public License, was used for curve fitting.

The quality of fitting was tested with 2 different criteria, namely, correlation coefficient, R^2 , and Root Mean Square Error, RMSE. It should be noted that a value of R^2 closer to 1 and RMSE closer to 0 indicates better fit.

The *GAB equation* was used to model water desorption of different type of rice is as follows:

$$m = \frac{m_0 c k a_w}{(1 - k a_w)(1 - k a_w + c k a_w)} \quad (1)$$

where c , k are GAB constants and m_0 is the monolayer moisture content.

The RMSE was calculated as follows:

$$RMSE = \sqrt{\frac{\sum_{i=1}^N (m_e^i - m_p^i)^2}{N}} \quad (2)$$

where m_e is the experimental value, m_p is the predicted value, and N is the number of experimental data.

It was observed GAB equation could not describe the curves when water activity ranged from 0 to 0.979, except for the husk of the rice. However, when water activity range was narrowed to 0.2-0.8 or 0.2-0.97, GAB equation gave sufficient accuracy to describe the desorption isotherms for all types of rice for each variety. The constants of GAB equation and the curve fitting quality are tabulated in Table 3.

Table 3. Values of the parameters of desorption curves for GAB model

Rice Type	Model Values			Statistical Values	
	m_0	c	k	R^2	RMSE
M202-R*	9.670	108.89	0.632	0.997	0.393
M206-R**	11.06	88.43	0.558	0.998	0.251
M202-B**	9.398	118.23	0.639	0.996	0.414
M206-B**	13.051	14.01	0.497	1.0	0.000
M202-W**	11.90	14.71	0.543	0.998	0.322
M206-W*	10.31	89.97	0.694	0.991	1.061
M202-H***	9.753	21.56	0.599	0.969	1.587
M206-H***	11.98	40.87	0.567	0.884	3.210

*: Valid in the range of 0.2-0.97 water activity

**: Valid in the range of 0.2-0.8 water activity

***: Valid in the range of 0-0.979 water activity

It is known that the GAB isotherm equation is an extension of the two-parameter (m_0 , c) BET model, taking into account the modified properties of the sorbate in the multilayer region through the introduction of a third parameter, namely k . Most of the values in the literature fall into the narrow range of 0.56 to 1.00 depending on water activity range and temperature (Chirife et al., 1992). The k values reported by Gencturk *et al.* (1986) was in the range of 0.64 to 0.75 for wild rice at 10.0 and 43.5°C. On the contrary, Togrul and Arslan (2006) reported a k value in the range of 0.002 to 0.672 for long commercial class, ‘Baldo’ type rice (*Oryza sativa L.*). However, in this study the values for M202 and M206 variety fell into the range of 0.497 to 0.694. The difference in range observed in this study could be due to rice variety, the temperature studied and the water activity range that the fitting was performed.

It is observed from Table 3 that GAB equation gave sufficient accuracy to describe the desorption isotherms of M202 and M206. Therefore, GAB model can be used to describe desorption isotherms of M202 and M206.

Distribution of carbohydrates, lipids and proteins in rice kernels

Scanning electron microscopy (SEM) was used to determine the distribution of carbohydrates, lipids and proteins in rice kernels. In order to take SEM images, whole rice kernels were cut in longitudinal planes with a razor blade. The kernel pieces were mounted such that the middle portion of the grain was facing up onto aluminum specimen stubs with double-adhesive coated carbon tabs (Ted Pella, Redding, CA). The mounted specimens were coated with gold-palladium in a Denton Desk II sputter (Denton Vacuum, LLC., Moorestown, NJ) coating unit. The samples were observed and photographed in a Hitachi S-4700 field emission scanning electron microscope (Hitachi, Japan). Leica MZ16F stereo microscope equipped with fluorescence was used to view the carbohydrate, lipid and protein distribution of rice kernels. Whole rice grains were encased in paraffin. Sections were made at 10 μm on a Leica RM22056 rotary microtome. The sections were collected with tape and mounted onto slides (Ogawa et al., 2003). In order to view lipid distribution sections were stained with 0.05% aqueous Nile Blue A for 1 min and observed immediately using a fluorescence filter set for blue excitation (Excitation: 450-490 nm, Barrier: Long Pass 515 nm). Lipids appear yellow to orange under the mentioned conditions. In order to view carbohydrates and proteins sections were stained Periodic Acid-Schiff's (Clark,

1981) and 0.0001% Light Green in 1% acetic acid and observed under bright field conditions. Sample images are shown in Figure 12 and Figure 13.

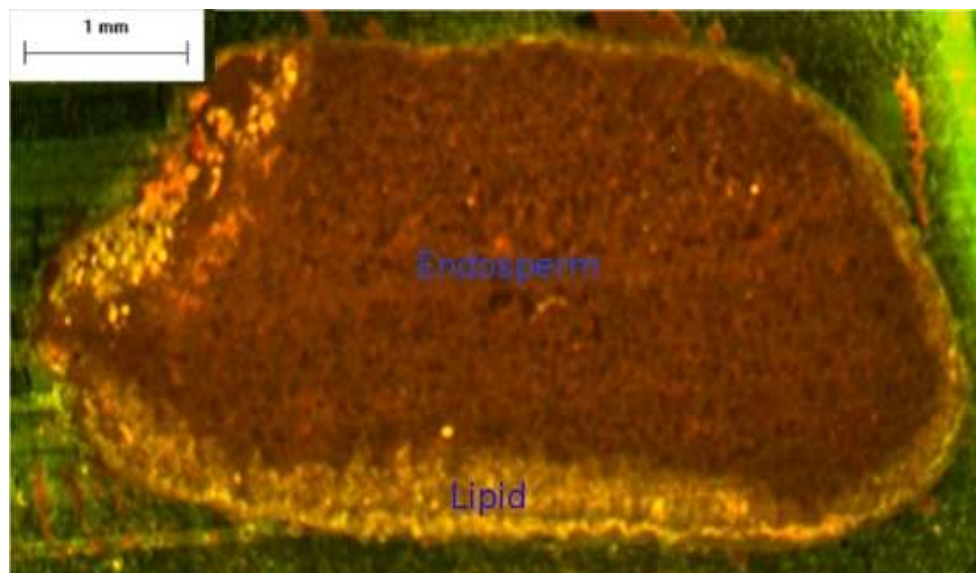


Figure 12. Microscopy image showing carbohydrates and lipids in M206 rice kernel

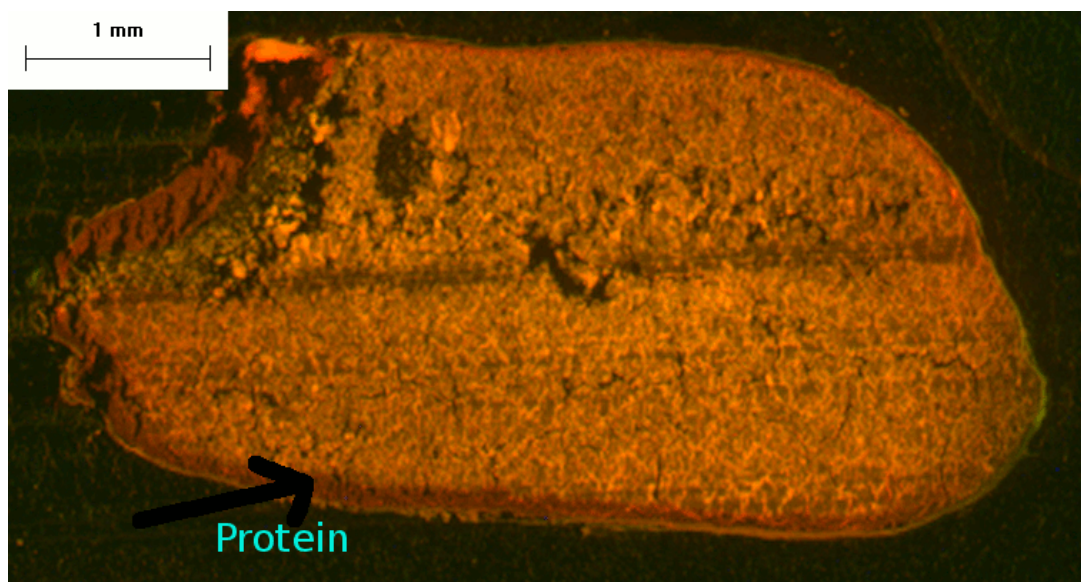


Figure 13. Microscopy image showing proteins in M206 rice kernel

The scanned images were analyzed using GIMP 2.6.7 (GNU Image Manipulation Program) distributed under GNU General Public License.

As seen in Figure 12 and Figure 13, a 1 mm length marker was placed on the images by the SEM instrument's software. The corresponding pixel counts were found using GIMP's measurement tool. Then at least 5 measurements were made at each side of the components layer, such as the lipid layer in Figure 12, and the average thicknesses in pixels were converted to corresponding millimeters. By cross-sectioning rice into several slices, we analyzed the thickness of lipid, carbohydrate and protein using at least 4 different images from corresponding slices. As shown

in Figure 16, the rice kernel was divided into 4 different regions, namely top, bottom, left and right. The thicknesses of each component are shown in Table 4.

Table 4. Thicknesses of different components of rice of M206

Component	Thickness (mm)			
	Top	Bottom	Left	Right
<i>Lipid</i>	0.141 ± 0.053	0.259 ± 0.059	0.130 ± 0.075	0.269 ± 0.030
<i>Protein</i>	0.137 ± 0.020	0.246 ± 0.156	0.073 ± 0.030	0.093 ± 0.041
<i>Carbohydrate</i>	2.193 ± 0.213		1.014 ± 0.110	

It should be noted that the thickness reported for carbohydrate is the length of major and minor axis for top-to-bottom and left-to-right, respectively, should cross-section of rice be considered as an ellipse. The standard deviation in the reported values is partly caused due to the staining technique, where in some occasions the stain of one component might diffuse into other components and therefore showing the color of the diffusing component and also partly caused due to heterogeneous distribution of components within different cross-sections.

In the future, the similar data presented in Table 4 can also be obtained for other rice varieties and compared with each other, which may explain the fissuring resistance of some varieties in terms of their chemical composition.

Structure of rice kernel

Rice structure was visualized by scanning electron microscopy. Transverse cut of the kernel is shown in Figure 14. It reveals that there is a gap between husk and the brown rice. To confirm that this gap is not due to cutting procedures involved in taking SEM images, we took X-ray images of intact rice kernels, as shown in Figure 15.

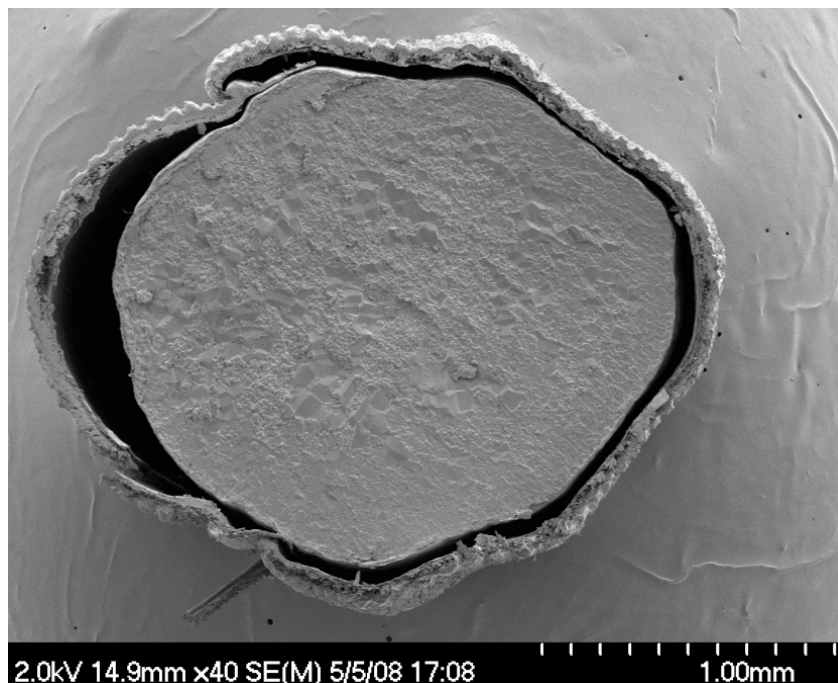


Figure 14. SEM image of transverse cut of the rice kernel

For X-ray imaging, wet and dry kernels of rice varieties M202 and M206 were used. Rice kernels were placed on an eight inch diameter ring-tray lined with a Rubbermaid brand transparent contact sheet. The tray was then placed on an x-ray film holder enclosing a 35 cm by 43 cm Kodak industrex CX sheet of ISO 9002 x-ray film. The rice samples were then x-rayed for two minutes at 17 kV in a Hewlett Packard faxitron series X-Ray cabinet (model #43804N) equipped with a beryllium window (0.25mm) x-ray tube. The X-Ray film was then developed using a Kodak X-OMAT 2000 Processor. The developed film was then scanned at a resolution of 1200 dpi using a Microtek Scan Maker 9800XL scanner. The scanned images, shown in Figure 15, were analyzed using GIMP 2.6.7. Since the force exerted by the caliper may compress the gap between brown rice and husk and also the porous structure of husk and therefore may cause error, instead of measuring the dimensions of rough rice, in order to get actual size of length and width, a caliper was used to measure the dimensions of each brown rice x-rayed. Then using the measurement tool of GIMP, the pixel counts corresponding to height and length were found for each rice kernel, which was averaged and expressed in pixel/mm. The gap between brown rice and husk was measured in pixels and was then converted to mm. The awn of the rice husk was considered to be the top and the values were reported for top, bottom, left and right as shown in Figure 16. For each side at least 3 measurements were made using the measurement tool of GIMP and average values are reported.

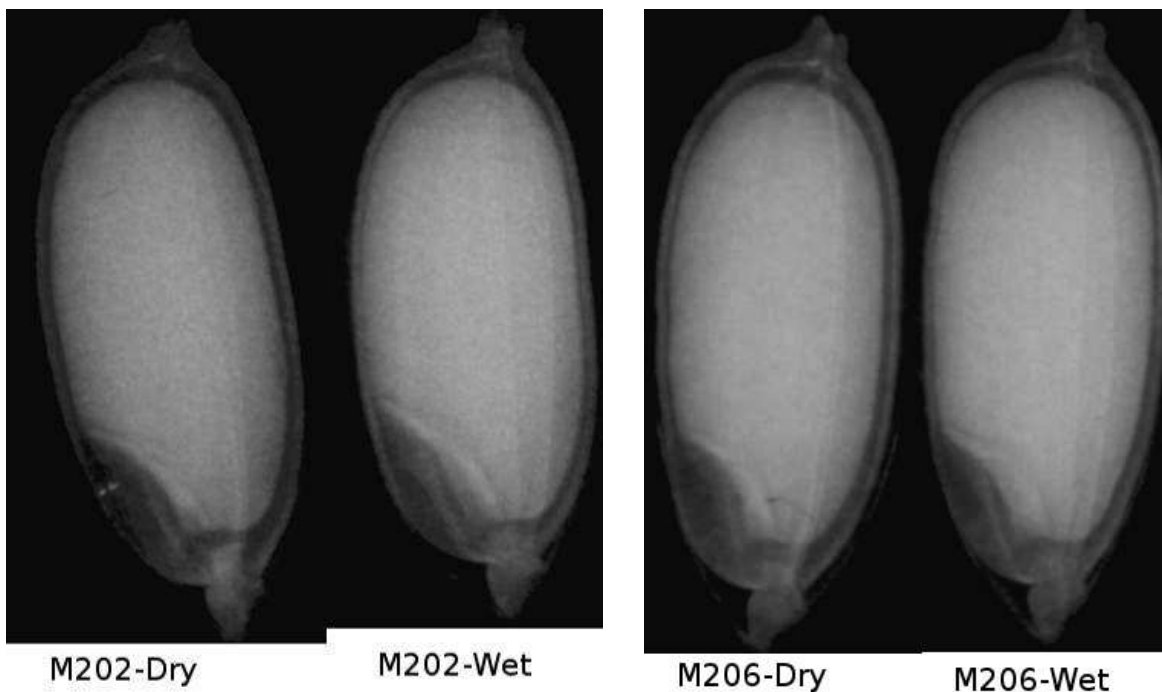


Figure 15. Selected kernels from X-ray image of rough rice of M202 and M206 varieties

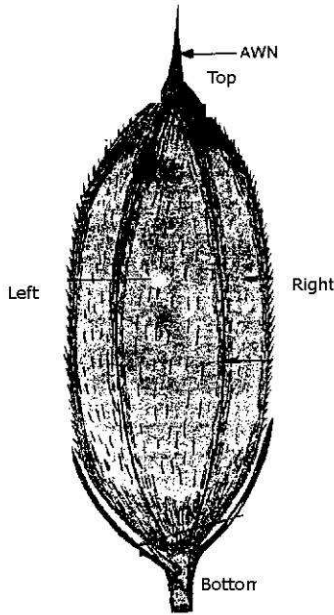


Figure 16. The orientation of rice kernel

The thickness of the gap between the husk and brown rice for M202 and M206 is shown in Table 5. It is seen that in all cases the thickness of the gap is less than 0.1 mm and that the gap was thicker for dry rice than the wet rice for M202 and M206. It is also worth to mention that the gap thickness was larger for the top and bottom sides than the left and right sides.

Table 5. Thickness of the gap between husk and brown rice for M202 and M206

Component	Thickness (mm)			
	Top	Bottom	Left	Right
<i>M202 – Dry</i>	0.062 ± 0.010	0.069 ± 0.014	0.023 ± 0.010	0.027 ± 0.006
<i>M202 – Wet</i>	0.034 ± 0.028	0.062 ± 0.026	0.014 ± 0.012	0.015 ± 0.009
<i>M206 – Dry</i>	0.050 ± 0.011	0.070 ± 0.017	0.020 ± 0.010	0.026 ± 0.010
<i>M206 – Wet</i>	0.043 ± 0.013	0.051 ± 0.011	0.019 ± 0.009	0.018 ± 0.007

REFERENCES

- Arlabosse, P., Rodier, E., Ferrasse, J.H., Chavez, S. and Lecomte, D. (2003). Comparison between static and dynamic methods for sorption isotherm measurements. *Drying Technology*, **21**(3), 479-497.
- Brunauer, S., Deming, L.S., Deming, W.E. and Troller, E. (1940). On the theory of Van der Waals adsorption of gases. *Journal of American Society*, **62**, 1723-1732.
- Chirife, J., Timmermann, E.O., Iglesias, H.A. and Boquet, R. (1992). Some features of the parameter k of the GAB equation as applied to sorption isotherms of selected food materials. *Journal of Food Engineering*, **15**, 75-82.
- Gencturk, M.B., Bakshi, A.S., Hong, Y.C. and Labuza, T.P. (1986). Moisture transfer properties of wild rice. *Journal of Food Process Engineering*, **8**, 243-261.

Roman-Gutierrez, A.D., Guilbert, S. and Cuq, B. (2002). Distribution of Water between Wheat Flour Components: A Dynamic Water Vapour Adsorption Study. *Journal of Cereal Science*, 36(3), 347-355.

Togrul, H. and Arslan, N., (2006). Moisture sorption behaviour and thermodynamic characteristics of rice stored in a chamber under controlled humidity. *Biosystems Engineering*, **95(2)**, 181-195.

CONCISE GENERAL SUMMARY OF CURRENT YEAR'S RESEARCH

Broken or fissured rice reduces the crop value significantly. Understanding mechanism of fissuring is key to develop fissure resistant rice varieties and better drying methods. Moisture absorption by kernels in humid environment and moisture gradients produced during the drying process are believed to be the main causes of kernel fissuring. To study this, we have measured moisture distribution inside the kernel during drying process and compared the differences in moisture absorption properties of two popular Californian rice varieties M202 and M206. We also determined structure and distribution of carbohydrates, lipids and proteins of rice varieties.

To see the moisture distribution inside the rice kernel, we used Magnetic Resonance Imaging (MRI) method. We observed that moisture removal is larger in regions near embryo or germ during first two hours of drying. This trend was identified in drying at 20, 25 and 43 °C. To confirm this observation, direct moisture measurement method such as oven drying will be used.

To compare drying rates of varieties M202 and M206, we dried them in column dryer at 25 and 43 °C. Drying rates of two varieties were found similar. Absorption property of different rice components, namely rough rice, brown rice, white rice and husk was determined using Dynamic Vapor Sorption (DVS) method. Among the different components, order of absorption rate is husk > white rice > brown rice > rough rice. M202 rice variety was observed to absorb moisture faster than M206 variety. This could be among the possible reasons of higher resistance of M206 to fissuring than M202. The moisture absorption data was used to develop a model to predict equilibrium moisture content of these rice components at different relative humidity environments. Rice components from variety M202 were found to have lower equilibrium moisture contents than rice variety M206.

Procedure to determine the distribution of carbohydrates, lipids and proteins in kernel by Scanning Electron Microscopy (SEM) was developed. In M206 kernel, lipids and protein were observed to be located in germ and bran region while most of carbohydrates are found in endosperm region. In the future, distribution of carbohydrates, lipids and proteins in M202 variety will also be determined and compared with M206 to identify the differences that might affect their absorption and fissure resistance properties. During SEM imaging, rice kernels were found to consist a small gap between husk and brown rice. To confirm existence of this gap, X-ray imaging was used. It was observed that dry rice kernels have bigger gap than wet ones and size of gap is highest on top and bottom of kernel.

In this study, we used advanced techniques such as MRI, DVS, SEM, X-ray imaging to determine structure, chemical distribution, absorption properties and moisture distribution in rice kernels. These methods have resulted in understanding fissure formation phenomena better and will help in developing fissure-resistant rice varieties.

PUBLICATIONS OR REPORTS

N/A

ACKNOWLEDGEMENT

The investigators would like to express their appreciation for the great support received from the following personnel and organization

Gokhan Bingol

Bhagwati Prakash

De Wood

Tina Williams

Jeff Walton

Gary Schmidt

UC Davis

USDA-ARS-WRRC

Farmer's Rice Cooperative